ACS OMEGA

http://pubs.acs.org/journal/acsodf

Article

Structure–Property Relationships of Dibenzylidenecyclohexanones

Marina V. Fomina,* Sergey Z. Vatsadze, Alexandra Ya. Freidzon, Lyudmila G. Kuz'mina, Anna A. Moiseeva, Roman O. Starostin, Vyacheslav N. Nuriev, and Sergey P. Gromov*

Cite This: *ACS Omega* 2022, 7, 10087–10099

Read Online

ACCESS | Metrics & More | Article Recommendations | Supporting Information

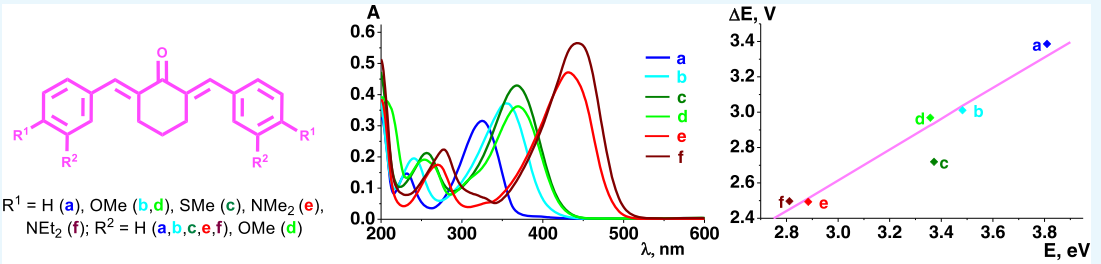

ABSTRACT: A series of symmetrical dibenzylidene derivatives of cyclohexanone were synthesized with the goal of studying the physicochemical properties of cross-conjugated dienones (ketocyanine dyes). The structures of the products were established and studied by X-ray diffraction, NMR spectroscopy, and electronic spectroscopy. All products had the *E,E*-geometry. The oxidation and reduction potentials of the dienones were determined by cyclic voltammetry. The potentials were shown to depend on the nature, position, and number of substituents in the benzene rings. A linear correlation was found between the difference of the electrochemical oxidation and reduction potentials and the energy of the long-wavelength absorption maximum. This correlation can be employed to analyze the properties of other compounds of this type. The frontier orbital energies and the vertical absorption and emission transitions were calculated using quantum chemistry. The results are in good agreement with experimental redox potentials and spectroscopic data.

1. INTRODUCTION

The enormous synthetic potential of the carbon–carbon double bond conjugated with the carbonyl group has long and successfully been utilized in organic chemistry.[1,2] The introduction of two double bonds in conjugation with the keto group enables some additional transformations.[3] These compounds, called cross-conjugated dienones, ketocyanine dyes, or (more rarely) diarylidene derivatives of ketones, attract the attention of researchers due to diverse synthetic chemistry and extensive scope of applicability, first of all, in biology and medicine.[4−6] Recently, cross-conjugated dienones with pyridine substituents have started to be used as ligands for the preparation of discrete and polymeric coordination compounds.[7−9]

Apart from participating in addition reactions, the dienone double bonds account for two more features of this class of compounds. First, an intrinsic feature of dienones is that they exist as *E*- and *Z*-isomers, with interconversion between them being induced by various factors such as light, acids, and complex formation with transition metals.[10−14] Most often, *E,E*-isomers are most stable for cyclopentanone and cyclohexanone derivatives. The percentage of *E,Z*- and *Z,Z*-isomers increases with increasing ring size.[4,12]

One more important feature of carbonyl-conjugated double bonds is the ability to undergo [2+2]-photocycloaddition (PCA) reactions.[12,15,16] Furthermore, in the case of free dienones, transformations of this type can occur both in the crystal and in solution. The possibility and stereoselectivity of PCA can both be controlled by supramolecular preorganization of double bonds, i.e., by creating the most appropriate geometry of the preceding dimer.[17−19] In the case of pyridine derivatives in the crystal, this can be accomplished by supramolecular templating by metal complexes,[20] resorcinol (pyridine-containing monoenones[21] and acyclic dienones[22]) or by treatment with silver ions (only pyridine-containing acyclic dienones were studied).[23]

Within the framework of the project on the design of photoswitchable supramolecular systems, we started a comprehensive targeted investigation of cross-conjugated dienones containing ionophoric substituents such as crown ethers.[24] The idea of this study was to generate hybrid molecules combining two functional components: an ionophoric group capable of coordination to metal ions,

Received: November 1, 2021
Accepted: February 23, 2022
Published: March 14, 2022

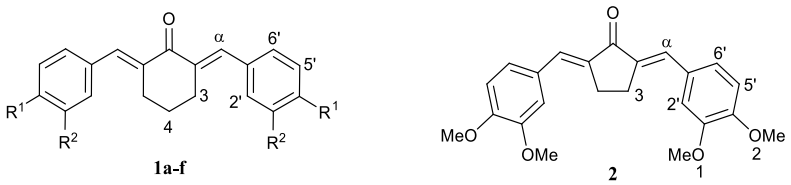

1: R^1 = H (**a**), OMe (**b,d**), SMe (**c**), NMe_2 (**e**), NEt_2 (**f**); R^2 = H (**a-c,e,f**), OMe (**d**)

Figure 1. Structure of compounds **1a−f** and **2**.

ammonium ions, or other analytes and a photoswitchable group providing control of the coordination by exposure to external light. For a more in-depth understanding of the photochemical reactions that take place, it is necessary to study in detail the properties and physicochemical characteristics of model compounds. In addition, it is necessary to establish the possibility of conducting the PCA reaction in the crystal and in solution without supramolecular preorganization of the reacting double bonds (Figure 1).

Here, we report the synthesis and study of dienones **1a−f**, which differ in the nature and the number of alkylthio, dialkylamino, and alkoxy substituents. These structures are chromophoric models of crown ethers and aza/thia-crown ethers. As the central moiety, we choose cyclohexanone to draw an analogy with cyclopentanone derivative **2** addressed in our previous study.[25]

The structures of compounds were established by X-ray diffraction analysis and were studied by NMR spectroscopy and electronic spectroscopy. An X-ray diffraction study was used to find out how favorable the double bonds of neighboring molecules are arranged for PCA to occur in the crystal without a supramolecular action. Cyclic voltammetry (CV) measurements were carried out to find the oxidation and reduction potentials, which were used to elucidate the dependence of the energy characteristics of molecules on the position, nature, and number of substituents in the benzene rings. Also, we attempted to find a correlation between the photophysical and electrochemical characteristics of dienones **1a−f**.

2. RESULTS AND DISCUSSION

2.1. Synthesis. Compounds **1a−f** and **2** were synthesized by alkaline aldol condensation of cyclohexanone and cyclopentanone, respectively, with two equivalents of substituted benzaldehyde (Claisen−Schmidt reaction, Scheme 1), similar to published procedures.[12,25−29]

All compounds **1a−f** were isolated as brightly colored crystalline solids. All dienones were found to exist as *E,E*-isomers, as can be drawn from the data of NMR spectroscopy. Indeed, the chemical shifts of the olefinic protons of dienones **1a−f**, occurring in the 7.51−7.60 ppm range, correspond to the *E,E*-isomers.[12]

Scheme 1. Synthesis of Dienones 1a−f and 2

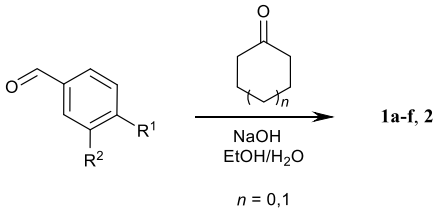

2.2. X-ray Diffraction Analysis. For compounds **1**, except for **1f**, X-ray diffraction data were obtained. X-ray diffraction studies confirmed the NMR data, indicating the formation of *E,E*-isomers of the dienone molecules. The structures of the molecules are depicted in Figure 2.

The crystals of **1c** and **1d** have two crystallographically independent molecules (**1c**-1 and **1c**-2 or **1d**-1 and **1d**-2).

In the molecules, the central six-membered ring has the half-chair conformation with five carbon atoms and oxygen atoms lying in a plane and the C4 (C4B) atom significantly displaced from this plane. All of the molecules have a flattened shape, and only structure **1e** occupying a special position in the crystal unit cell adopts a strictly planar structure. A twist of the benzene rings with respect to the −C═C−C(O)−C═C system may reach rather essential values. The corresponding dihedral angles are 26.8(1) and 39.1(1)° in **1a**, 10.4 and 24.4° in **1b**, 14.1(5) and 12.5(5)° in one independent molecule and 23.8(6) and 23.1(6)° in another one of **1c**, and 19.1(2) and 31.1(2)° as well as 23.3(2) and 21.9(2)° in both independent molecules of **1d**.

Selected geometric parameters of the molecules are summarized in Table 1.

The data of Table 1 attest to the similarity of the most important geometric parameters of molecules **1a−e** containing a six-membered ring as the central part of the molecule. In particular, in all of these molecules, the exocyclic C2−C7 and C6−C7A double bonds are substantially localized (bond d3 in Table 1) and the 1-2-3-4 moieties are approximately planar; the torsion angles given in the table are grouped around values of 180 or 0°. The molecules are somewhat strained, which is manifested as a systematic increase in the ω4-5 and, especially, ω3-4 bond angles, and decrease in the ω2-3 bond angles. These data indicate that π-conjugation is retained over the whole 4-3-2-1-2-3-4 moiety, despite the indicated noticeable localization of double bond d3.

Although flattened, the considered molecules are generally nonplanar. This prevents the stacking arrangement of the molecules in the crystal, which is important for the possibility of the [2+2]-photocycloaddition reaction in the solid state.[30] Apparently, the [2+2]-photocycloaddition reaction of compounds **1a−e** in the solid state requires the use of a supramolecular template.

Quantum chemical calculations for the structures are consistent with X-ray diffraction data. The 5-4-3-2 torsion angle is 25° in **1a**, 21−23° in **1b−d**, and 16−17° in **1e,f**. This correlates with the electron-donating ability of the substituents.

2.3. NMR Spectroscopy. NMR spectroscopy can be used to determine the fine structure of organic molecules and their assemblies in solutions.[31] It is not always possible to compare NMR data, characterizing the structure of molecules in

https://doi.org/10.1021/acsomega.1c06129
ACS Omega 2022, 7, 10087−10099

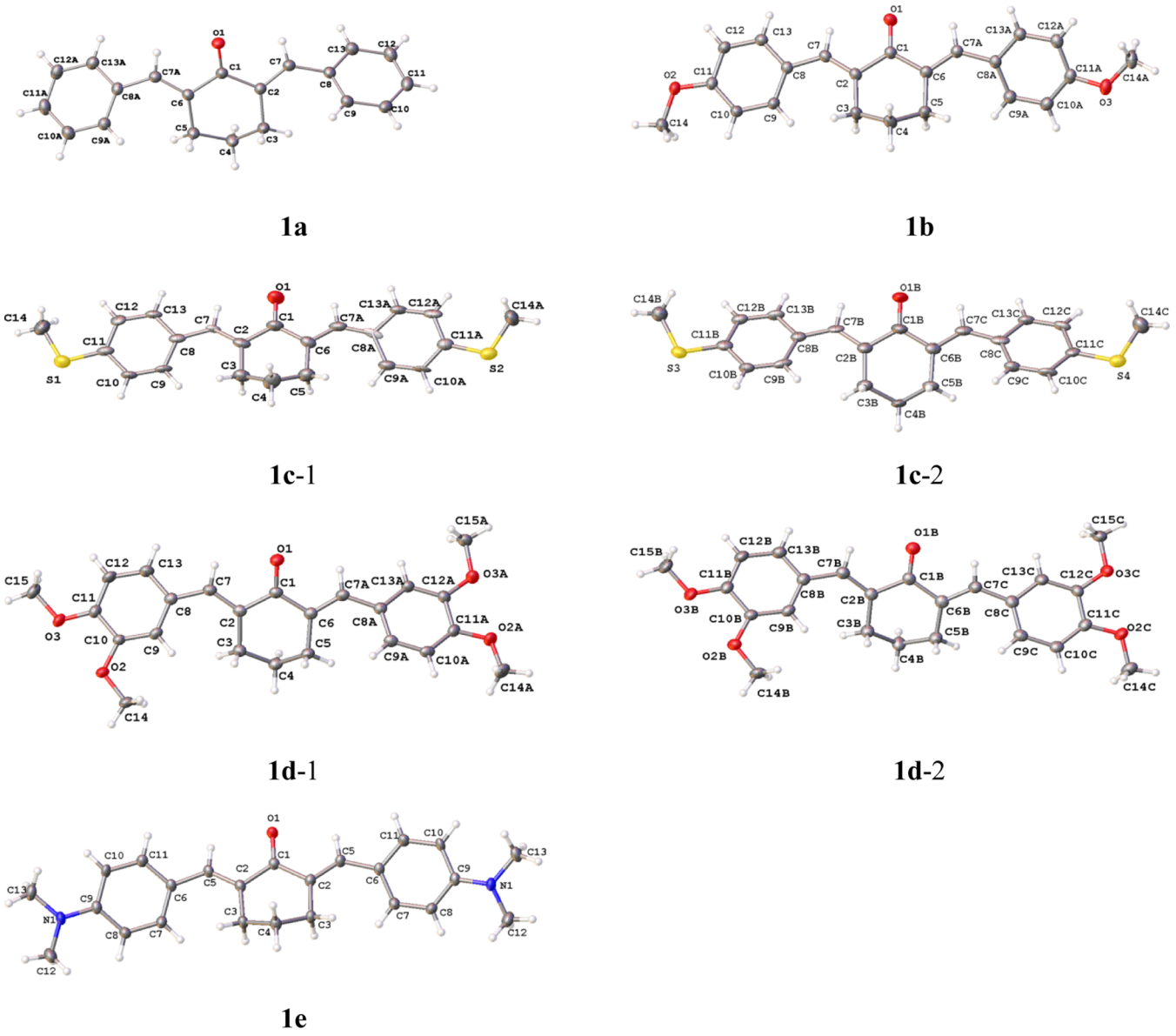

Figure 2. Molecular structure and atom numbering for crystals of **1a**−**e**.

solution with crystallographic data for the whole series, since the crystals of high quality are not available for all compounds. In the case of dienones, it is especially important to explore their conformational behavior in solutions, which is important for prediction and determination of the structures of supramolecular systems based on bis-crown-containing dienones.[24] Therefore, we studied the structural characteristics of (*E*,*E*)-dienones **1d** and **2** using various NMR techniques.

In the crystalline state, (*E*,*E*)-tetramethoxydienone **1d** and (*E*,*E*)-tetramethoxydienone **2**[32] exist as nearly planar unsymmetrical *syn*,*anti*- and symmetrical *syn*,*syn*-conformers, respectively, which is apparently caused by the requirement for close packing of molecules. On going to solutions, fast conformational equilibrium between symmetrical *syn*,*syn*-, *anti*,*anti*-, and unsymmetrical *syn*,*anti*-conformers may be established (Figure 3) by analogy with the previously studied bis-crown-containing stilbenes and distyrylbenzenes.[33,34]

The nuclear Overhauser effect spectroscopy (NOESY) spectra of compounds **1d** and **2** in CD_2Cl_2, which are shown in Figures S1 and S2 (the atom numbering differing from the IUPAC rules is presented in Figure 1), exhibit averaged signals from various conformers. The spectrum of dienone **1d** displays an intense cross-peak, corresponding to the intramolecular through-space interaction between the H(2′) protons of the benzene ring and the H(3) methylene protons of the cyclohexanone moiety, and a weak cross-peak between the H(6′) aromatic protons and the H(α) protons of ethylene bonds. These types of coupling are inherent in the *syn*,*syn*-conformer. Apart from the indicated cross-peaks, a cross-peak between the H(6′) aromatic protons and the H(3) methylene protons of the cyclohexanone moiety is present in the NOESY spectrum. However, it is worth mentioning that the spectrum does not show a cross-peak between the H(2′) protons of the benzene ring and the H(α) protons of the ethylene bonds (Figure S1). The absence of this cross-peak in the spectrum can be explained by assuming that mainly *syn*,(*syn*/*anti*)-conformers are involved in equilibrium. The contribution of H(2′)−H(α) coupling in the *syn*,*anti*-conformer to the overall spectral pattern is lower, as only one of the two H(α) protons of the ethylene bond is coupled with H(2′).

https://doi.org/10.1021/acsomega.1c06129
ACS Omega 2022, 7, 10087−10099

Table 1. Selected Geometric Parameters (Bond Length *d*, Å; Bond Angle *ω*, deg, and Torsion Angle *τ*, deg) for the Molecules of 1a−e

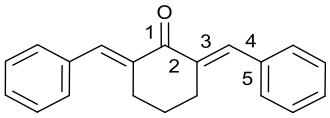

parameter	1a	1b	1c[a]	1d[a]	1e
d1	1.230(1)	1.231(1)	1.232(9)	1.240(2)	1.228(5)
			1.235(9)	1.227(2)	
d2	1.498(1)	1.502(1)	1.493(11)	1.499(3)	1.495(3)
	1.501(1)	1.502(2)	1.519(11)	1.491(3)	1.495(3)
			1.496(11)	1.502(3)	
			1.490(11)	1.499(3)	
d3	1.344(1)	1.352(2)	1.334(10)	1.343(3)	1.345(3)
	1.348(1)	1.350(2)	1.351(11)	1.345(3)	
			1.371(10)	1.347(3)	
			1.373(11)	1.346(3)	
d4	1.470(1)	1.461(1)	1.453(10)	1.461(3)	1.462(3)
	1.468(1)	1.462(1)	1.358(11)	1.459(3)	
			1.443(10)	1.463(3)	
			1.434(11)	1.458(3)	
***ω*1-2**	120.07(9)	120.75(9)	120.9(7)	120.1(2)	120.85(15)
	120.97(9)	120.37(9)	119.1(7)	120.2(2)	
			120.2(7)	120.3(2)	
			120.6(7)	121.1(2)	
***ω*2-3**	116.3(8)	115.47(9)	117.6(6)	116.7(2)	116.8(2)
	115.34(9)	116.50(9)	118.1(7)	117.3(2)	
			116.0(7)	116.3(2)	
			116.2(6)	116.1(2)	
***ω*3-4**	128.92(9)	132.1(1)	133.1(6)	130.9(2)	130.6(2)
	130.17(9)	130.2(1)	134.3(7)	129.7(2)	
			132.3(6)	130.7(2)	
			131.1(6)	130.4(2)	
***ω*4-5**	122.57(9)	126.19(9)	127.0(7)	124.7(2)	125.7(2)
	124.67(9)	125.36(9)	127.3(7)	123.8(2)	
			125.3(6)	124.2(2)	
			125.2(7)	125.8(2)	
***τ*1-2-3**	−18.9(1)	6.8(2)	7(1)	3.7(3)	−4.5(3)
	11.0(1)	2.5(2)	−6(1)	−9.6(3)	4.5(3)
			8(1)	−5.5(3)	
			−9(1)	7.6(3)	
***τ*2-3-4**	177.5(1)	178(1)	179.6(1)	−179.8(2)	179.4(2)
	177.8(1)	180(1)	179.5(8)	176.1(2)	
			−172.8(7)	−176.5(2)	
			174.1(8)	179.4(2)	

[a]Data are given for two independent molecules.

The NOESY spectrum of dienone **2** showed similar interactions: intense cross-peaks corresponding to the intramolecular coupling of the H(2′) and H(6′) protons of the benzene ring with the H(3) methylene protons of the cyclopentanone moiety and the cross-peak between the H(6′) aromatic protons and the H(*α*) protons of the ethylene bonds (Figure S2).

Although the NOESY spectra do not make it possible to accurately determine the contribution of each conformer of **1d** and **2** to the equilibrium due to the strong coupling of methylene protons with both H(2′) and H(6′) type protons in all conformers, the spectral details still provide the conclusion that a mixture of *syn*,(*syn*/*anti*)-conformers is present predominantly.

An indirect indication of the predominance of *syn*,(*syn*/*anti*)-conformers in solution can also be derived from a comparison of the positions of signals for the H(2′) and H(6′) benzene protons, which are located in the *ortho*-position to the ethylene substituent. The H(2′) type protons are also located in the *ortho*-position to the electron-donating methoxy group and, in principle, should resonate in a higher field than H(6′) located in the *para*-position.

The theoretical ratio between three possible conformers for each dienone was calculated from the energies of the stable structures of these compounds found using the FireFly software package (Figure 3).

The ^{1}H NMR spectra of conformers of (*E*,*E*)-dienones **1d** and **2**, calculated with allowance for their mole fractions, are in good agreement with experimental data (Table 2), in

https://doi.org/10.1021/acsomega.1c06129
ACS Omega 2022, 7, 10087−10099

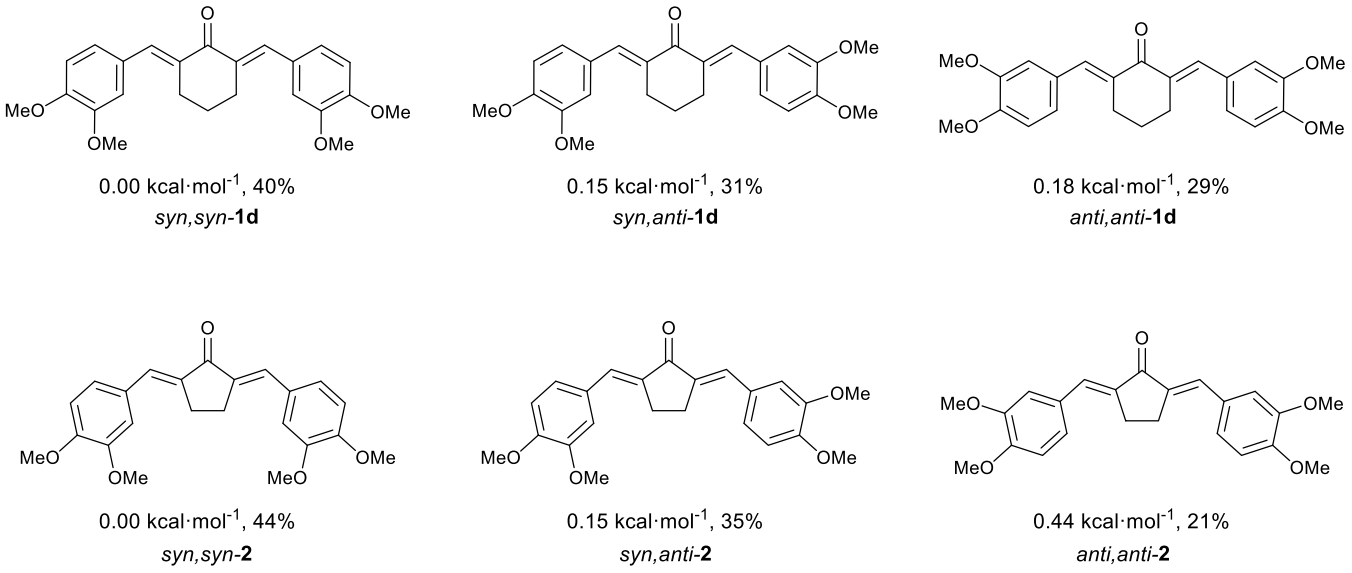

Figure 3. Possible conformers of (*E*,*E*)-dienones **1d** and **2** and stability of conformers relative to the most favorable *syn*,*syn*-conformers (for compounds **1d** and **2**, respectively). The mole fractions of the conformers at room temperature in MeCN are given in percent; the values were found by the Boltzmann equations using relative energies of the conformers.

particular, the H(2′) *ortho*-proton has a greater chemical shift than the H(6′) *ortho*-proton. Thus, quantum chemical data are in good agreement with the experimental data.

Table 2. Proton Chemical Shifts of Compounds 1d and 2 Averaged Taking into Account the Mole Fractions of Conformers in Comparison with Experimental Data (in MeCN-d_3)

	1d		**2**	
	δ, ppm			
protons	experiment	calculation	experiment	calculation
C(4)H2	1.82	1.92		
C(3)H2	2.98	3.22	3.15	3.25
H(5′)	7.00	6.84	7.05	6.87
H(2′)	7.14	7.32	7.26	7.22
H(6′)	7.17	7.75	7.28	7.39
CHAr (α)	7.66	8.36	7.44	7.74

2.4. Electrochemistry. With the goal to elucidate the effect of substituents in the aromatic rings of cyclohexanone-based cross-conjugated dienones on the energy of frontier orbitals and to compare the results with these parameters of cyclopentanone-based dienones described previously,[25] we studied compounds **1a**–**f** by cyclic voltammetry (CV) on a cleaned glassy carbon (GC) electrode in MeCN solutions. The CV curves were measured from 0 V toward the cathode or anode potential region. Table 3 presents the first peak potentials determined in MeCN to compare the electrochemical parameters with the data obtained by other physicochemical methods in the same solvent. The table also presents the differences (shifts) of the reduction and oxidation potentials of the substrates in comparison with unsubstituted compound **1a**.

We calculated the vertical ionization potentials (IPs) and electron affinities (EAs) of the dyes. We have found that electron detachment takes place from the highest occupied molecular orbital (HOMO) − 1, while the electron attachment occurs to the lowest unoccupied molecular orbital (LUMO). The IPs and EAs are also given in Table 3. The values correlate with the oxidation and reduction potentials and well reproduce the trend in the series (shift with respect to **1a**).

The first cathodic peaks of compounds **1a**–**f** are single electron and are irreversible, but the reverse peak current is markedly lower (Figure 4a). The cathodic peak potentials of cyclohexadienones are shifted to the cathodic side compared to the potentials of the corresponding substituted cyclopentadienones,[25] which may be indicative of a lower degree of conjugation between C═O and C═C fragments of

Table 3. Electrochemical Potentials of Compounds 1a–f ($C = 1 \times 10^{-4}$ mol L^{-1}) in MeCN Measured by CV Relative to Ag/AgCl/KCl (sat.) in the Presence of 0.1 M Bu_4NClO_4 on a GC Electrode (Potential Sweep Rate of 200 mV s^{-1}) and Frontier Orbital Energies Calculated by Quantum Chemistry

	R^1, R^2	E_{red}, V	EA, eV	ΔE_{red}, mV (ΔEA)[a]	E_{ox}, V	IP, eV	ΔE_{ox}, mV (ΔIP)[b]	$\Delta E = E_{ox} - E_{red}$, V	EA–IP, eV
1a	H, H	−1.38	2.642	0	2.02	6.291	0	3.40	3.649
1b	OMe, H	−1.51	2.513	130 (129)	1.52	5.840	500 (451)	3.03	3.327
1c	SMe, H	−1.39	2.618	10 (24)	1.33	5.724	690 (567)	2.72	3.106
1d	OMe, OMe	−1.46	2.524	80 (118)	1.53	5.695	490 (596)	2.99	3.171
1e	NMe2, H	−1.63	2.316	250 (326)	0.87	5.098	1150 (1193)	2.50	2.782
1f	NEt2, H	−1.64	2.304	260 (338)	0.86	5.059	1160 (1232)	2.50	2.755

[a]Shift of the reduction potentials relative to those of **1a**. [b]Shift of the oxidation potentials relative to those of **1a**.

https://doi.org/10.1021/acsomega.1c06129
ACS Omega 2022, 7, 10087−10099

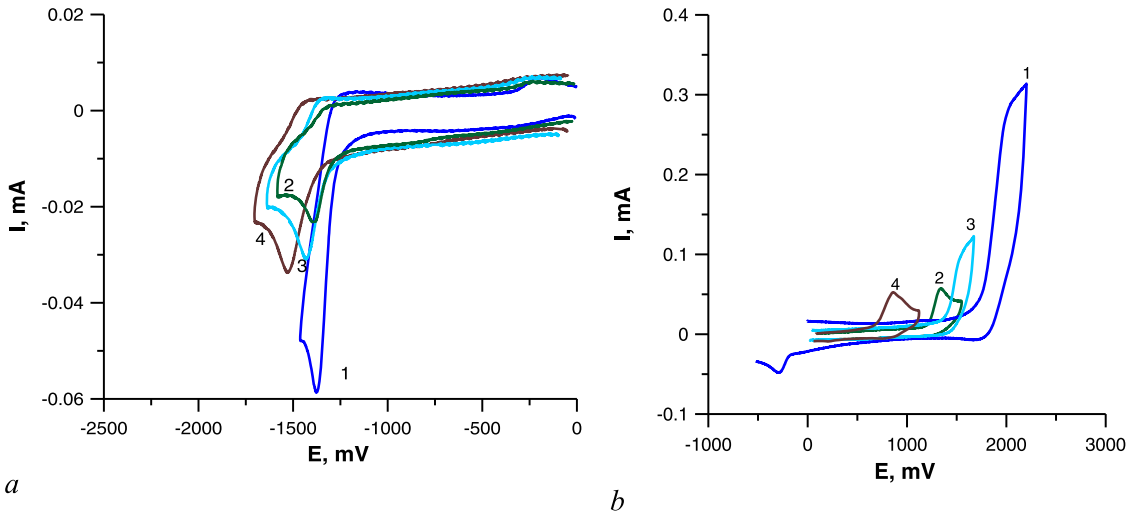

Figure 4. Voltammetric curves for the reduction (a) and oxidation (b) of dienones: (1) **1a**, (2) **1c**, (3) **1b**, and (4) **1f**.

dibenzylidenecyclohexanone derivatives compared to analogous cyclopentanone derivatives.

The range of differences between the first cathodic peak potentials of dienones **1b**–**f** and unsubstituted dienone **1a** is rather broad (−10 to 260 mV, Table 3 and Figure 4a). The most pronounced and comparable effects on the cathodic potentials are made by electron-donating dimethyl- and diethylamino groups: the potentials of **1e** and **1f** shift to the cathodic region by 250 and 260 mV, respectively. The effects of one and two methoxy groups in this series are much less pronounced (130 and 80 mV, respectively). The methylthio group exerts a negligibly low electron-donating effect (10 mV).

The effect of substituents on the electrooxidation of dienones **1b**–**f** in comparison with unsubstituted **1a** was much more pronounced. The potential shifts to the less anodic region were 490−1150 mV (Table 3; see Figure 4b). The most pronounced shift was observed for dienones **1e** and **1f** containing dimethyl- and diethylamino groups; the oxidation potentials of these compounds were close to the corresponding values for amines (0.8−1.1 V).[35]

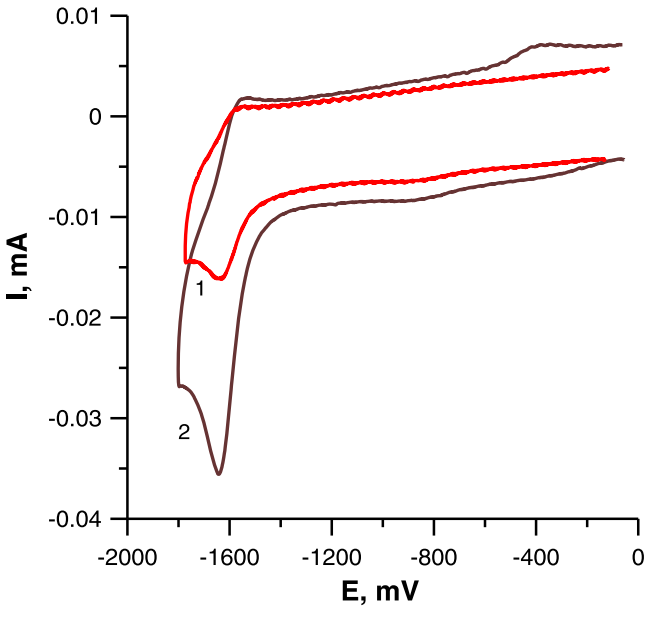

Figure 5. Voltammetric curves of the reduction of dienones: (1) **1e** and 2 (**1f**).

These considerable differences between the anodic potentials of substituted dienones **1b**–**f** and unsubstituted dienone **1a** indicate that the HOMO and HOMO − 1 are more localized on the electron-donating substituents of the conjugated π-system (see Figures S3–S7 of the Supporting Information).

Comparison of the electrochemical behaviors of dibenzylidene-substituted cyclopentanone[25] and cyclohexanone derivatives containing *para*-dimethylamino groups in benzene rings revealed the shift of the first reduction peaks to a more cathodic region (−1.38 and −1.63 V, respectively). This fact attests to a decrease in the degree of π-conjugation on going from the five-membered to the six-membered ring. In less conjugated compound **1e**, the electron density is localized to a higher extent on the dimethylamino group, and oxidation occurs at a lower anodic potential. For compounds with a five-membered ring, the anodic potential increases with increasing degree of conjugation (0.87 and 0.93, respectively) due to increasing transfer of π-electron density toward the carbonyl group. It is worth noting that dimethyl- and diethylamino-dibenzylidenecyclohexanone derivatives **1e** and **1f** are reduced at virtually identical potentials (Figure 5), whereas, for more conjugated cyclopentanone analogues, the difference between the cathodic potentials is 150 mV.[25]

2.5. Photophysics. With the goal of determining the effect of substituents on the spectral properties of dienones, we recorded the electronic absorption and fluorescence spectra of **1a**–**f** (Table 4 and Figure 6).

All dienones show an intense long-wavelength absorption band (LAB) (λ_{max} from 326 nm for **1a** to 445 nm for **1f**) and several more bands at shorter wavelengths. The LABs can be assigned to HOMO−LUMO type transitions,[36,37] and the shorter-wavelength bands correspond to local electron transitions within the aromatic rings. Note the qualitative dependence of the LAB maximum position on the electron-donating ability of the *para*-substituents in benzylidene moieties. The LAB of *para*-dialkylamino-substituted **1e**,**f** is most red-shifted relative to that of unsubstituted **1a**, which is in good agreement with the high electron-donating ability of substituents and correlates with the lowest (among the given series of compounds) oxidation potentials (Table 3). In the

https://doi.org/10.1021/acsomega.1c06129
ACS Omega 2022, 7, 10087−10099

Table 4. Parameters of the Electronic Absorption and Fluorescence Spectra of Dienones 1a−f in MeCN

	λ_{abs} (ε)/nm ($mol^{-1}\cdot dm^3\ cm^{-1}$)		λ_{fl}/nm	
dienone	experiment	calculation (oscillator strength)	experiment	calculation (oscillator strength, τ_{rad}, ns)
1a	326 (31 500)	381 (0.03)		1736 (0.005, 8826)
		355 (0.99)		
1b	356 (37 000)	390 (1.14)		848 (0.03, 323)
1c	368 (43 000)	417 (1.27)		620 (0.11, 51)
1d	370 (36 000)	411 (1.10)		878 (0.03, 414)
1e	431 (45 400)	454 (1.53)	563	478 (1.61, 2)
1f	445 (56 000)	461 (1.64)	562	485 (1.71, 2)

Table 5. Relative Energies of (*E,E*), (*E,Z*), and (*Z,Z*) Isomers of the Dienones 1a−f in the S1 State

dienone	(*E,E*)	(*E,Z*)	(*Z,Z*)
1a	0.00	−6.00	−1.44
1b	0.00	−4.86	−0.96
1c	0.00	−2.22	0.92
1d	0.00	−6.98	−1.66
1e	0.00	5.39	6.15
1f	0.00	5.45	6.15

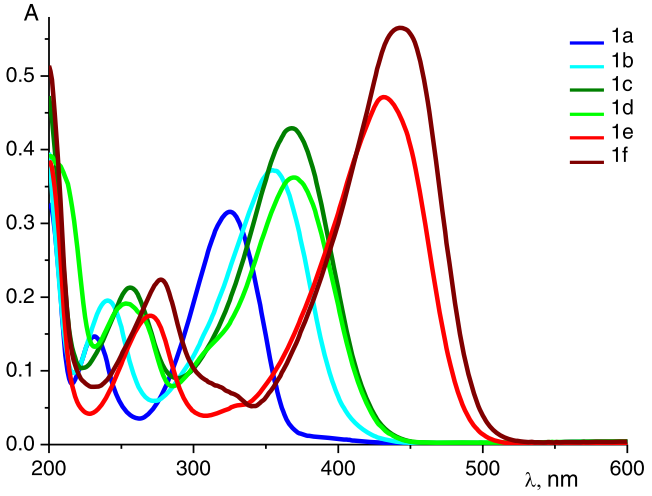

Figure 6. Absorption spectra of dienones **1a−f**, in MeCN, $C = 1 \times 10^{-5}$ mol L^{-1}.

case of *meta*-methoxy-substituted compound **1d**, the LAB maximum shifts to 370 nm, and the oxidation potential increases with respect to those of **1e,f**. In dienone **1c**, the SMe group has an even lower electron-donating ability, which reasonably induces a further short-wavelength shift of the LAB maximum and increase in E_{ox}.

The simulated absorption spectra are in qualitative agreement with the experimental results and reproduce the trend in this series. The first electron transition has the $\pi-\pi^*$ nature (HOMO−LUMO) for all dyes, except **1a**. In **1a**, the first transition has the $n-\pi^*$ nature (HOMO − 2−LUMO) and is dark. The corresponding orbitals are depicted in Figure 7. Generally, the blue-shifted LABs of dienones **1a−f** compared with the cyclobutanone[38] and cyclopentanone[25] derivatives are attributable to lower planarity of the π system of cyclohexanones.

The fluorescence of the dyes deserves a special discussion. Unlike cyclobutanone and cyclopentanone dyes,[39] only **1e** and **1f** show noticeable fluorescence. Our calculations explain this fact (Table 5). Our calculations show that, unlike the ground state, the excited S1 state is not always dominated by the (*E,E*) isomers. Only in **1e** and **1f**, (*E,E*) isomer has the lowest energy in the S1 state, with (*E,Z*) and (*Z,Z*) isomers lying noticeably higher. This means that the excited **1e** and **1f** relax to their (*E,E*) isomers, which emit at 478 and 485 nm, respectively, with high oscillator strengths and, therefore, short radiative lifetimes (2 ns). In other dienones, the excited state is dominated by the (*E,Z*) isomer with small oscillator strength and long radiative lifetime (from 51 ns and more). Such long radiative lifetime allows the molecule to relax nonradiatively. Obviously, the barrier from the (*E,E*) to (*E,Z*) isomer is sufficiently small so that the isomerization proceeds rather fast.

Characteristic features of the absorption and emission of compound **1f** and its aza-crown ether analogue are described in our publication.[40]

2.6. Correlations. Previously, we studied the dependences of a number of calculated and experimental characteristics for a broad range of *N*-donor ligands, including some pyridine-containing dienones. In particular, we identified a linear dependence between the electrochemical and spectrophotometric characteristics of dienone molecules.[41,42]

Here, we performed a correlation analysis (Figure 8) between the energy of the long-wavelength absorption maximum and the oxidation/reduction potential difference to reveal the possible correlation of the electrochemical and optical data with the electronic properties of substituents in the benzene rings of **1a−f**.

The observed correlation is not surprising because both oxidation/reduction involves frontier orbitals, and excitation LAB is a HOMO−LUMO transition. Our direct calculations of vertical ionization potential and electron affinity show that the electron is attached to LUMO, while electron detachment takes place from HOMO − 1, which is quasi-degenerate with HOMO. We note the fact that solvation slightly affects the correlations between the redox and optical properties. Although the effect of solvation is different for the excitation energy, IP, and EA, the solvation effects in the series differ slightly, which retains the correlation.

These results indicate that, despite the irreversibility of electrochemical reduction, the energy characteristics of the frontier orbitals in a series of related compounds such as cross-conjugated dienones can be adequately described by both electrochemical and spectrophotometric data. The results of this study could be useful for analysis of new dienone-type compounds and for the design of required characteristics of molecules.

3. CONCLUSIONS

The products of cyclohexanone condensation with benzaldehyde derivatives tend to exist as *E,E*-isomers. The conformational analysis of (*E,E*)-dienones using X-ray diffraction and

https://doi.org/10.1021/acsomega.1c06129
ACS Omega 2022, 7, 10087−10099

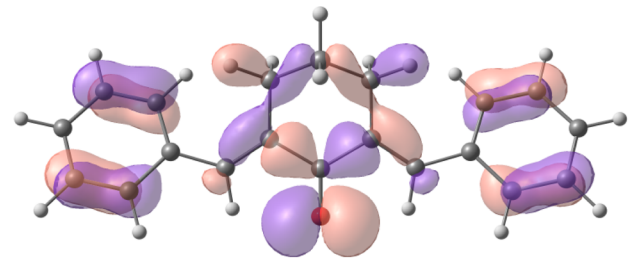

n orbital (HOMO-2) of dienone **1a**

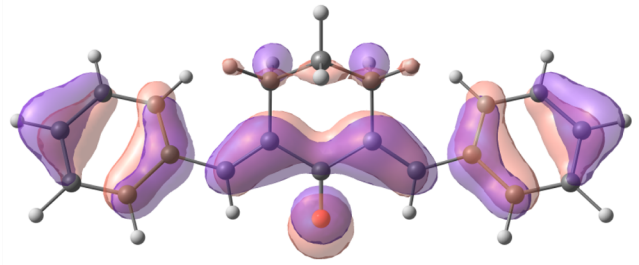

π orbital (HOMO-1) of dienone **1a**

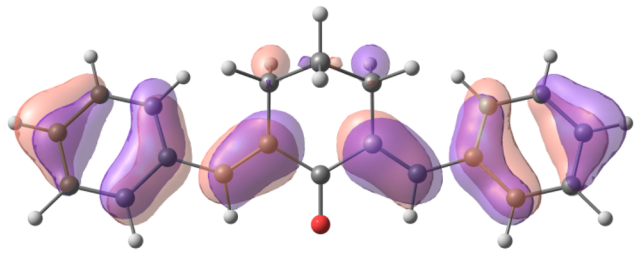

π orbital (HOMO) of dienone **1a**

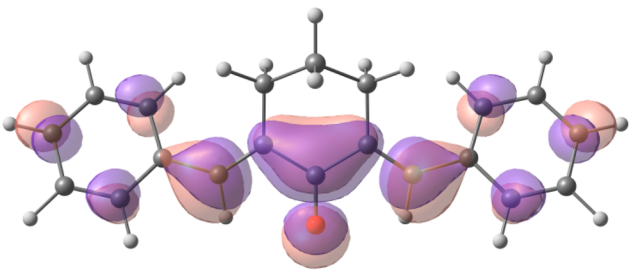

π^* orbital (LUMO) of dienone **1a**

Figure 7. Orbitals involved in the first electron transition of dienone **1a**, oxidation and reduction.

NMR data revealed their structural features in the crystalline state and in solution. More favorable *syn*,(*syn*/*anti*)-conformations of the conjugated moieties of dibenzylidenecyclohexanones containing four methoxy groups were confirmed by quantum chemical calculations. It was found that the solid-state PCA reaction of compounds **1a**–**e** requires the use of a supramolecular template. The spectral properties of dienone derivatives **1a**–**f** were compared considering their electronic spectra. Using quantum chemical calculations, the absence of fluorescence of **1a** was explained by the fact that the lowest excited state of **1a** is n–π^* dark state, whereas in **1b**–**f**, it is

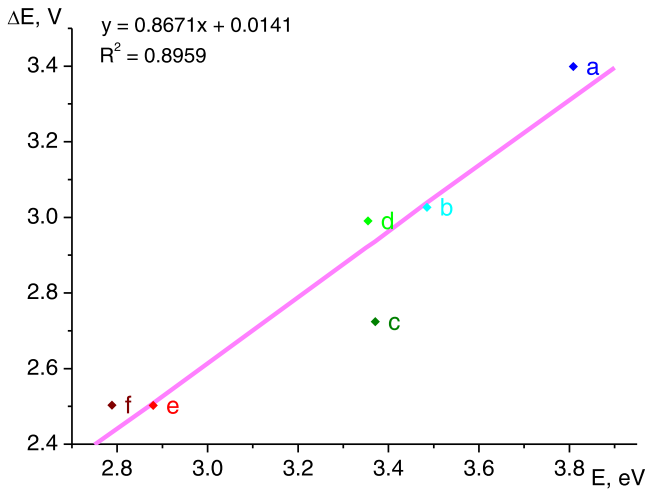

Figure 8. Correlation between the energy of the long-wavelength absorption maximum and the difference of oxidation/reduction potentials for dienones **1a**–**f**.

π–π^* bright state. The obtained dependences of the redox potentials on the position, nature, and number of substituents in the benzene ring and their correlation with photophysical and quantum chemical characteristics are useful for the subsequent studies of photoactive dienone derivatives. The structures and properties of cyclohexanone-based dienones can also be used to design photoactive supramolecular systems.

4. EXPERIMENTAL SECTION

4.1. Materials. MeCN (extra high purity, water content <0.3%, Cryochrom) was used to prepare solutions. Bu_4NClO_4 (≥99%, for electrochemical analysis) was purchased from Sigma-Aldrich and used as a background electrolyte. Cyclohexanone, cyclopentanone, benzaldehyde, 4-methoxybenzaldehyde, 3,4-dimethoxybenzaldehyde, 4-(methylthio)-benzaldehyde, 4-dimethylaminobenzaldehyde, and 4-diethylaminobenzaldehyde (Sigma-Aldrich) were used as received. EtOH (chemically pure) was used without additional purification, and (2*E*,6*E*)-2,6-bis(3,4-dimethoxybenzylidene)-cyclopentanone (**2**) was prepared as described previously.[25] DC-Alufolien Aluminiumoxid 60 F_{254} neutral was purchased from Merck.

*4.1.1. Synthesis of 2,6-Dibenzylidenecyclohexanone Derivatives **1a**–**f** (General Procedure).* Ethanol (1 mL) and a 10% aqueous solution of NaOH (1 mL) were mixed in a round-bottom flask. A mixture of aldehyde (2 mmol) and cyclohexanone (1 mmol) in EtOH (2 mL) was prepared separately, and a half of this mixture was added with vigorous stirring to the EtOH/NaOH (aq) solution. Fifteen minutes later, the other half of the aldehyde/cyclohexanone mixture was added. Stirring was continued until the reaction was over (thin-layer chromatography, TLC monitoring). The precipitate that formed was collected on a filter, thoroughly washed with an EtOH–water mixture (1:1 v/v), then with water and again with an EtOH–water mixture (1:1 v/v), and dried in air.

*4.1.1.1. (2E,6E)-2,6-Dibenzylidenecyclohexanone (**1a**).* Pale-yellow fine crystalline powder. Yield: 90%, mp: 118–120 °C (cf. ref 26: 116–118 °C). ^{1}H NMR (δ, ppm, J/Hz): 1.80 (m, 2 H, C(4)H_2), 2.96 (m, 4 H, C(3)H_2, C(5)H_2), 7.38–7.41 (m, 4 H, 2 H(3′), 2 H(5′)), 7.47 (m, 2 H, 2 H(4′)), 7.55 (m, 4 H, 2 H(2′), 2 H(6′)), 7.72 (s, 2 H, 2 C*H*Ph). Calcd for $C_{20}H_{18}O$ (274.36): C, 87.56; H, 6.61.

https://doi.org/10.1021/acsomega.1c06129
ACS Omega 2022, 7, 10087–10099

Table 6. Crystallographic Characteristics and X-ray Experiment Details for 1a−c

dienone	1a	1b	1c
molecular formula	$C_{20}H_{18}O$	$C_{22}H_{22}O_3$	$C_{22}H_{22}OS_2$
molecular weight, g·mol^{-1}	274.34	334.40	366.51
crystal system	monoclinic	monoclinic	monoclinic
space group	$P2_1/c$	$P2_1/c$	$P2_1/n$
a, Å	9.4669(3)	8.8899(3)	9.2176(11)
b, Å	18.2488(7)	9.4022(3)	22.382(3)
c, Å	9.3371(3)	20.6943(7)	18.333(2)
α, deg	90.00	90.00	90.00
β, deg	115.2690(10)	100.1720(10)	103.619(2)
γ, deg	90.00	90.00	90.00
V, Å^3	1458.72(9)	1702.54(10)	3675.8(8)
Z	4	4	8
ρ_{calcd}, g·sm^{-3}	1.249	1.305	1.325
$F(000)$	584.0	712.0	1552.0
μ(Mo Kα), mm^{-1}	0.075	0.086	0.297
crystal size, mm	0.44 × 0.36 × 0.32	0.38 × 0.22 × 0.20	0.46 × 0.26 × 0.02
scan range on 2θ, deg.	4.76−58.00	4.66−58.00	2.92−52.00
index range	$-12 \le h \le 12$, $-24 \le k \le 24$, $-12 \le l \le 12$	$-12 \le h \le 12$, $-12 \le k \le 12$, $-28 \le l \le 28$	$-11 \le h \le 11$, $-27 \le k \le 27$, $-22 \le l \le 22$
number of measured refl.	14 940	18 436	30 107
number of independent refl. [$R_{(int)}$]	3830 [0.0240]	4522 [0.0266]	7225 [0.1062]
number of refl with $I > 2\sigma(I)$	3227	3697	3673
number of variables	190	228	455
R indices for $I > 2\sigma(I)$	$R_1 = 0.0403$, $wR_2 = 0.1082$	$R_1 = 0.0403$, $wR_2 = 0.1071$	$R_1 = 0.1075$, $wR_2 = 0.2960$
R indices for all refl.	$R_1 = 0.0483$, $wR_2 = 0.1122$	$R_1 = 0.0513$, $wR_2 = 0.1129$	$R_1 = 0.1898$, $wR_2 = 0.3240$
GOOF	1.061	1.037	1.062
residuals, min/max, e Å^{-3}	−0.23/0.32	−0.21/0.38	−0.48/1.11

https://doi.org/10.1021/acsomega.1c06129
ACS Omega 2022, 7, 10087−10099

Table 7. Crystallographic Characteristics and X-ray Experiment Details for 1d and 1e

dienone	1d	1e
molecular formula	$C_{24}H_{26}O_5$	$C_{24}H_{28}N_2O$
molecular weight, g·mol^{-1}	394.45	360.48
crystal system	monoclinic	orthorhombic
space group	$P2_1/n$	$Cmc2_1$
a, Å	8.6522(8)	21.798(4)
b, Å	32.232(3)	8.9774(16)
c, Å	14.3606(13)	9.6932(17)
α, deg	90.00	90.00
β, deg	97.169(2)	90.00
γ, deg	90.00	90.00
V, Å^3	3973.6(6)	1896.8(6)
Z	8	4
ρ_{calcd}, g·sm^{-3}	1.319	1.262
$F(000)$	1680.0	776.0
μ(Mo Kα), mm^{-1}	0.092	0.077
crystal size, mm	0.52 × 0.43 × 0.02	0.44 × 0.21 × 0.04
scan range on 2θ, deg	3.12−58.00	4.91−57.99
index range	$-11 \le h \le 11$, $-43 \le k \le 43$, $-19 \le l \le 19$	$-29 \le h \le 29$, $-12 \le k \le 12$, $-13 \le l \le 13$
number of measured refl.	43 363	9168
number of independent refl. [$R_{(int)}$]	10 564 [0.0732]	2730 [$R_{(int)}$ = 0.0557]
number of refl with $I > 2\sigma(I)$	6213	2076
number of variables	531	129
R indices for $I > 2\sigma(I)$	R_1 = 0.0595, wR_2 = 0.1271	R_1 = 0.0474, wR_2 = 0.1000
R indices for all refl.	R_1 = 0.1212, wR_2 = 0.1415	R_1 = 0.0762, wR_2 = 0.1138
GOOF	1.013	1.022
residuals, min/max, e Å^{-3}	−0.23/0.25	−0.24/0.17
flack parameter		−2(2)

Found: C, 87.74; H, 6.35. UV−vis (MeCN) λ_{max} 231 nm (ε = 14 700 M^{-1}·cm^{-1}), 326 nm (ε = 31 500 mol^{-1}·dm^3 cm^{-1}).

*4.1.1.2. (2E,6E)-2,6-Bis(4-methoxybenzylidene)-cyclohexanone (**1b**).* Yellow crystalline powder. Yield: 85%, mp: 157−159 °C (cf. ref 26: 156−158 °C). ^{1}H NMR (δ, ppm, J/Hz): 1.80 (m, 2 H, C(4)H$_2$), 2.94 (m, 4 H, C(3)H$_2$, C(5)H$_2$), 3.85 (s, 6 H, 2 MeO), 7.01 (d, 4 H, 2 H(3′), 2 H(5′), J = 8.8), 7.53 (d, 4 H, 2 H(2′), 2 H(6′), J = 8.8), 7.67 (s, 2 H, 2 CHAr). Calcd for $C_{22}H_{22}O_3$ (334.41): C, 79.02; H, 6.63. Found: C, 78.83; H, 6.79. UV−vis (MeCN) λ_{max} 241 nm (ε = 19 500 M^{-1}·cm^{-1}), 356 nm (ε = 37 000 mol^{-1}·dm^3 cm^{-1}).

*4.1.1.3. (2E,6E)-2,6-Bis[4-(methylthio)benzylidene]-cyclohexanone (**1c**).* Yellow crystalline powder. Yield: 82%, mp: 178−180 °C (cf. ref 26: 183−184 °C). ^{1}H NMR (δ, ppm, J/Hz): 1.81 (m, 2 H, C(4)H$_2$), 2.53 (s, 6 H, 2 MeS), 2.95 (m, 4 H, C(3)H$_2$, C(5)H$_2$), 7.33 (d, 4 H, 2 H(3′), 2 H(5′), J = 8.4), 7.49 (d, 4 H, 2 H(2′), 2 H(6′), J = 8.4), 7.66 (s, 2 H, 2 CHAr). Calcd for $C_{22}H_{22}OS_2$ (366.54): C, 72.09; H, 6.05. Found: C, 71.86; H, 6.17. UV−vis (MeCN) λ_{max} 256 nm (ε = 21 000 M^{-1}·cm^{-1}), 368 nm (ε = 43 000 mol^{-1}·dm^3 cm^{-1}).

*4.1.1.4. (2E,6E)-2,6-Bis(3,4-dimethoxybenzylidene)-cyclohexanone (**1d**).* Yellow fine crystalline powder. Yield: 83%, mp: 145 °C (cf. ref 27: 135−137 °C). ^{1}H NMR (δ, ppm, J/Hz): 1.82 (m, 2 H, C(4)H$_2$), 2.98 (m, 4 H, 2 C(3)H$_2$), 3.86 and 3.87 (s, 12 H, 2 3′-MeO, 2 4′-MeO), 7.00 (d, 2 H, 2 H(5′), J = 8.2), 7.14 (d, 2 H, 2 H(2′), J = 1.5), 7.17 (dd, 2 H, 2 H(6′), J = 8.2, J = 1.5), 7.66 (s, 2 H, 2 CHAr). Calcd for $C_{24}H_{26}O_5$ (394.46): C, 73.08; H, 6.64. Found: C, 72.79; H, 6.78. UV−vis (MeCN) λ_{max} 253 nm (ε = 19 000 M^{-1}·cm^{-1}), 370 nm (ε = 36 000 mol^{-1}·dm^3 cm^{-1}).

*4.1.1.5. (2E,6E)-2,6-Bis[4-(dimethylamino)benzylidene]-cyclohexanone (**1e**).* Yellow-orange fine crystalline powder. Yield: 52%, mp: 218−220 °C (cf. ref 28: 240−242 °C). ^{1}H NMR (δ, ppm, J/Hz): 1.73 (m, 2 H, C(4)H$_2$), 2.94 (m, 4 H, C(3)H$_2$, C(5)H$_2$), 3.01 (s, 12 H, 4 Me), 6.78 (d, 2 H(3′), 2 H(5′), J = 9.0), 7.47 (d, 4 H, 2 H(2′), 2 H(6′), J = 9.0), 7.62 (s, 2 H, 2 CHAr). Calcd for $C_{24}H_{28}N_2O$ (360.49): C, 79.96; H, 7.83; N, 7.77. Found: C, 79.78; H, 7.71; N, 7.57%. UV−vis (MeCN) λ_{max} 270 nm (ε = 17 400 M^{-1}·cm^{-1}), 431 nm (ε = 45 400 mol^{-1}·dm^3 cm^{-1}); fluorescence (MeCN, λ_{ex} 428 nm) λ_{max}^{fl} 563 nm.

*4.1.1.6. (2E,6E)-2,6-Bis[4-(diethylamino)benzylidene]-cyclohexanone (**1f**).* Dark orange crystalline powder. Yield: 12%, mp: 167−170 °C (cf. ref 29: 144−145 °C). ^{1}H NMR (δ, ppm, J/Hz): 1.17 (t, 12 H, 4 Me, J = 7.1), 1.82 (m, 2 H, C(4)H$_2$), 2.84 (m, 4 H, C(3)H$_2$, C(5)H$_2$), 3.44 (q, 8 H, 4 CH$_2$Me, J = 7.1), 6.75 (d, 4 H, 2 H(3′), 2 H(5′), J = 8.9), 7.44 (d, 4 H, 2 H(2′), 2 H(6′), J = 8.9), 7.60 (s, 2 H, 2 CHAr). Calcd for $C_{28}H_{36}N_2O$ (416.60): C, 80.73; H, 8.71; N, 6.72; Found: C, 80.56; H, 8.75; N, 6.62%. UV−vis (MeCN) λ_{max} 276 nm (ε = 22 300 M^{-1}·cm^{-1}), 445 nm (ε = 56 000 mol^{-1}·dm^3 cm^{-1}); fluorescence (MeCN, λ_{ex} 440 nm) λ_{max}^{fl} 562 nm.

4.2. Methods. The reactions were monitored by thin-layer chromatography using DC-Alufolien Aluminiumoxid 60 F_{254} neutral plates, Merck. Melting points (uncorrected) were measured on a Mel-Temp II instrument. ^{1}H NMR spectra were recorded on a Bruker DRX-500 spectrometer (operating at 500.13 MHz) in MeCN-d_3 at 25−30 °C using the solvent signal as the internal standard (δ_H 1.96 ppm). The chemical shifts were determined with an accuracy of 0.01 ppm, and the spin−spin coupling constants were determined with an accuracy of 0.1 Hz.

https://doi.org/10.1021/acsomega.1c06129
ACS Omega 2022, 7, 10087−10099

The electronic absorption spectra were measured on a Cary 4000 spectrophotometer in MeCN. Fluorescence spectra were obtained on a Cary Eclipse spectrofluorimeter at room temperature. All manipulations with solution dyes **1a**−**f** were performed in a darkroom under red light (daylight induces the *E*−*Z* photoisomerization).

4.3. Cyclic Voltammetry. The electrochemical measurements were carried out using an IPC_Pro M potentiostat in a three-electrode system. A glassy carbon disk (d = 2 mm) served as the working electrode, a 0.1 M Bu_4NClO_4 solution in MeCN was used as the supporting electrolyte, and Ag/AgCl/KCl (aq, sat.) reference electrode and a platinum plate auxiliary electrode were used. The working electrode surface was polished by alumina powder with a particle size of less than 0.5 μm (Sigma-Aldrich). In the CV measurements, the potential sweep rate was 100 mV s^{-1}. The potentials are presented with *iR*-compensation. The number of transferred electrons was determined by comparing the peak current in the substrate and the current of single-electron oxidation of ferrocene taken in the same concentration. Concentration of compounds **1a**, **1b**, **1c**, **1e**, and **1f** was 1×10^{-4} M.

4.4. X-ray Diffraction Experiments. A suitable single crystal of each of compounds **1a**−**e** was mounted on a CCD SMART APEX-II diffractometer under a stream of cooled nitrogen, and crystallographic parameters and X-ray reflection intensities were measured (Mo Kα radiation (λ = 0.71073 Å), graphite monochromator, ω-scan mode). Reduction of the experimental data was performed using a SAINT program.[43]

The structures were solved by direct methods and refined by least squares on F^2 in the anisotropic approximation for nonhydrogen atoms. The hydrogen atom positions were calculated geometrically and refined, at the final stage, using the riding model.

Crystallographic characteristics and structure refinement details are summarized in Tables 6 and 7.

The calculations were performed using OLEX-2 and SHELXTL-Plus software.[44,45] The X-ray diffraction studies were done at the Center for Collective Use of the Kurnakov Institute of General and Inorganic Chemistry, Russian Academy of Sciences. Structural data were deposited with the Cambridge Crystallographic Data Centre with numbers 1892893 (**1a**), 1892905 (**1b**), 2121817 (**1c**), 1892908 (**1d**), and 2121818 (**1e**).

4.5. Density Functional Theory (DFT) Calculations. The structure and energies of the molecules were calculated using density functional theory (DFT) with the PBE0 functional and 6-31+G(d,p) basis set using a FireFly program[46] partially based on the GAMESS code.[47] The solvent (acetonitrile) effects for the absorption spectra were taken into account using the dielectric polarizable continuum model (DPCM).[48] The vertical absorption and emission spectra were calculated by the time-dependent DFT (TDDFT) with the same functional, basis set, and solvent model. Vertical absorption spectra were calculated by TDDFT after geometry optimization of the ground state with DFT, while vertical emission spectra were calculated in a similar way after geometry optimization of the π−π^* excited state using the TDDFT and SMD[49] solvent model implemented in GAMESS. The radiative lifetimes were calculated using the given formula:

$$k_r = \frac{2}{3} f_{0i} \nu_{i0}^2;\ \tau_r = 1/k_r$$

We considered (*E*,*E*), (*E*,*Z*), and (*Z*,*Z*) isomers of dyes **1a**−**f** and **2**. We have found that (*E*,*E*) isomers have the lowest energy and make up >99.9% of the isomer mixture. The spectral and ionization properties were calculated only for the (*E*,*E*) isomer.

Dyes **1d** and **2** are capable of free rotation around C4−C5 bond. The mole fractions of the three possible rotamers of dienones **1d** and **2** were calculated using the partition function

$$x_i = \frac{e^{-E_i/kT}}{\sum_j e^{-E_j/kT}}$$

where x_i is the mole fraction of the ith conformer and E_i is the ground state energy of this conformer. The calculated UV−vis absorption and emission properties of the rotamers are almost the same (within 2 nm); therefore, we give only the values for the lowest energy conformer in the respective state: (*syn*,*syn*)-conformer for the absorption from the ground state and (*anti*,*anti*)-conformer for the emission from the S1 excited state.

The vertical ionization potentials (IPs) and electron affinities (EAs) were calculated by restricted open-shell DFT (RO-DFT) for the corresponding monocation and monoanion of each dye. The functional, basis set and solvation model were the same.

^{1}H NMR spectra were calculated using a Priroda program package[50,51] with the PBE functional and triple-ζ quality basis set. The optimized geometries were taken from the PBE0/6-31+G(d,p)/DPCM calculation. Previously,[52] we have shown that for dienones, solvent effects are important to properly reproduce the structures and conformation energies.

■ ASSOCIATED CONTENT

Supporting Information

The Supporting Information is available free of charge at https://pubs.acs.org/doi/10.1021/acsomega.1c06129.

Crystallographic data (CIF)
Crystallographic data (CIF)
Crystallographic data (CIF)
Crystallographic data (CIF)
Crystallographic data (CIF)
NOESY spectra of compounds **1d** and **2** in CD_2Cl_2 (Figures S1 and S2); cyclic voltammogram **1a** (Figure S3); fluorescence spectra of compounds **1e**,**f** (Figure S4); quantum chemical calculations, orbitals involved in the first electron transition of compounds **1b**−**f** (Figures S5−S9); and correlations between the calculated frontier orbital energies, ionization potential and electron affinities, and experimental oxidation and reduction potentials (Figures S10−S12) (PDF)

■ AUTHOR INFORMATION

Corresponding Authors

Marina V. Fomina − *Photochemistry Center of RAS, FSRC "Crystallography and Photonics", Russian Academy of Sciences, Moscow 119421, Russian Federation;* orcid.org/0000-0001-9401-7118; Email: mv_fomina@mail.ru

Sergey P. Gromov − *Photochemistry Center of RAS, FSRC "Crystallography and Photonics", Russian Academy of Sciences, Moscow 119421, Russian Federation; Department of Chemistry, M.V. Lomonosov Moscow State University,*

https://doi.org/10.1021/acsomega.1c06129
ACS Omega 2022, 7, 10087−10099

Moscow 119991, Russian Federation; orcid.org/0000-0002-2542-7807; Email: spgromov@mail.ru

Authors

Sergey Z. Vatsadze − *Department of Chemistry, M.V. Lomonosov Moscow State University, Moscow 119991, Russian Federation;* orcid.org/0000-0001-7884-8579

Alexandra Ya. Freidzon − *Photochemistry Center of RAS, FSRC "Crystallography and Photonics", Russian Academy of Sciences, Moscow 119421, Russian Federation;* orcid.org/0000-0002-7473-7692

Lyudmila G. Kuz'mina − *N.S. Kurnakov Institute of General and Inorganic Chemistry, Russian Academy of Sciences, Moscow 119991, Russian Federation*

Anna A. Moiseeva − *Department of Chemistry, M.V. Lomonosov Moscow State University, Moscow 119991, Russian Federation*

Roman O. Starostin − *Department of Chemistry, M.V. Lomonosov Moscow State University, Moscow 119991, Russian Federation*

Vyacheslav N. Nuriev − *Photochemistry Center of RAS, FSRC "Crystallography and Photonics", Russian Academy of Sciences, Moscow 119421, Russian Federation; Department of Chemistry, M.V. Lomonosov Moscow State University, Moscow 119991, Russian Federation*

Complete contact information is available at: https://pubs.acs.org/10.1021/acsomega.1c06129

Notes

The authors declare no competing financial interest.

■ ACKNOWLEDGMENTS

This work was supported by the Russian Science Foundation (project No. 19-13-00020, except synthesis). The synthesis of dienones **1a−f** was done under financial support of the Ministry of Science and Higher Education of the Russian Federation (State Assignment FSRC "Crystallography and Photonics" of RAS). The authors are grateful to Philip S. Zyuzkevich for his help in growing single crystals **1a−e** and Artem I. Vedernikov in interpreting the X-ray diffraction data. The calculations were performed using the computational facilities of the Joint Supercomputer Center of the Russian Academy of Sciences.

■ REFERENCES

(1) Ananikov, V. P.; Khemchyan, L. L.; Ivanova, Y. V.; Bukhtiyarov, V. I.; Sorokin, A. M.; Prosvirin, I. P.; Vatsadze, S. Z.; Medved'ko, A. V.; Nuriev, V. N.; Dilman, A. D.; Levin, V. V.; Koptyug, I. P.; Kovtunov, K. V.; Zhivonitko, V. V.; Likholobov, V. A.; Romanenko, A. V.; Simonov, P. A.; Nenajdenko, V. G.; Shmatova, O. I.; Muzalevskiy, V. M.; Nechaev, M. S.; Asachenko, A. F.; Morozov, O. S.; Dzhevakov, P. B.; Osipov, S. N.; Vorobyeva, D. V.; Topchiy, M. A.; Zotova, M. A.; Ponomarenko, S. A.; Borshchev, O. V.; Luponosov, Y. N.; Rempel, A. A.; Valeeva, A. A.; Stakheev, A. Yu.; Turova, O. V.; Mashkovsky, I. S.; Sysolyatin, S. V.; Malykhin, V. V.; Bukhtiyarova, G. A.; Terent'ev, A. O.; Krylov, I. B. Development of new methods in modern selective organic synthesis: preparation of functionalized molecules with atomic precision. *Russ. Chem. Rev.* **2014**, *83*, 885−985.

(2) *Organic Reactions, Volume 10*; Adams, R. V., Ed.; J. Wiley & Sons, Inc: New York, London, 1959; Vol. *10*, p 576.

(3) Vatsadze, S. Z.; Golikov, A. G.; Kriven'ko, A. P.; Zyk, N. V. Chemistry of cross-conjugated dienones. *Russ. Chem. Rev.* **2008**, *77*, 707−728.

(4) Cui, J.; Crich, D.; Wink, D.; Lam, M.; Rheingold, A. L.; Case, D. A.; Fu, W. T.; Zhou, Y.; Rao, M.; Olson, A. J.; Johnson, M. E.; et al. Design and synthesis of highly constrained factor Xa inhibitors: amidine-Substituted bis(benzoyl)-1,3-diazepan-2-ones and bis-(benzylidene)-bis(gem-dimethyl)cycloketones. *Bioorg. Med. Chem.* **2003**, *11*, 3379−3392.

(5) Jin, R.; Chen, Q.; Yao, S.; Bai, E.; Fu, W.; Wang, L.; Wang, J.; Du, X.; Wei, T.; Xu, H.; Jiang, Ch.; Qiu, P.; Wu, J.; Li, W.; Liang, G. Synthesis and anti-tumor activity of EF24 analogues as IKKβ inhibitors. *Eur. J. Med. Chem.* **2018**, *144*, 218−228.

(6) Cersosimo, U.; Sgorbissa, A.; Foti, C.; Drioli, S.; Angelica, R.; Tomasella, A.; Picco, R.; Semrau, M. S.; Storici, P.; Benedetti, F.; Berti, F.; Brancolini, C. Synthesis, Characterization, and Optimization for in Vivo Delivery of a Nonselective Isopeptidase Inhibitor as New Antineoplastic Agent. *J. Med. Chem.* **2015**, *58*, 1691−1704.

(7) Vatsadze, S. Z.; Kovalkina, M. A.; Sviridenkova, N. V.; Zyk, N. V.; Churakov, A. V.; Kuz'mina, L. G.; Howard, J. A. K. Novel dienone-based ligands for the synthesis of coordination polymers. *CrystEngComm* **2004**, *6*, 112−115.

(8) Vatsadze, S. Z.; Vatsadze, I. A.; Manaenkova, M. A.; Zyk, N. V.; Churakov, A. V.; Antipin, M. Yu.; Howard, J. A. K.; Lang, H. Three-coordinate silver(I) ions and tridentate ligands as complementary tectons in coordination polymer construction: a new example of semiregular 4.8(2) nets. *Russ. Chem. Bull.* **2007**, *56*, 1775−1781.

(9) Aly, A. A. M.; Vatsadze, S. Z.; Chernikov, A. V.; Walfort, B.; Rüffer, T.; Lang, H. A binuclear silver(I) perchlorate macrocycle based on 2,5-bis[(E)-(3-pyridyl)methylene]cyclopentanone: Crystal structure and solution behavior. *Polyhedron* **2007**, *26*, 3925−3929.

(10) Sanford, E. M.; Paulisse, K. W.; Reeves, J. T. A computational study of 2,5-dibenzylidenecyclopentanone and 2,6-dibenzylidenecyclohexanone, model compounds for poly(arylidenecycloalkanones). *J. Appl. Polym. Sci.* **1999**, *74*, 2255−2257.

(11) Grandeury, A.; Petit, S.; Coste, S.; Coquerel, G.; Perrio, C.; Gouhier, G. New synthesis of (Z,E)-2,7-bis(4-cyanobenzylidene)-cycloheptan-1-one under stereospecific constraints induced by host-guest interactions. *Chem. Commun.* **2005**, *41*, 4007−4009.

(12) Vatsadze, S. Z.; Manaenkova, M. A.; Sviridenkova, N. V.; Zyk, N. V.; Krut'ko, D. P.; Churakov, A. V.; Antipin, M. Yu.; Howard, J. A. K.; Lang, H. Synthesis and spectroscopic and structural studies of cross-conjugated dienones derived from cyclic ketones and aromatic aldehydes. *Russ. Chem. Bull.* **2006**, *55*, 1184−1194.

(13) Aizenshtat, Z.; Hausman, M.; Pickholtz, Y.; Tal, D.; Blum, J. Chlorocarbonylbis(triphenylphosphine)iridium-catalyzed isomerization, isoaromatization, and disproportionation of some cycloalkanones having exocyclic double bonds. *J. Org. Chem.* **1977**, *42*, 2386−2394.

(14) George, H.; Roth, H. J. Photoisomerisierung und Cyclo-1,2-Addition α,β-ungesättigter Cyclanone. *Tetrahedron Lett.* **1971**, *12*, 4057−4060.

(15) Kaupp, G.; Zimmermann, I. First Detection of a π-Coupled 1,5-Diradical via Cycloaddition. *Angew. Chem., Int. Ed.* **1981**, *20*, 1018−1019.

(16) Ovchinnikova, I. G.; Nikulov, D. K.; Bartashevich, E. V.; Matochkina, E. G.; Kodess, M. I.; Slepukhin, P. A.; Druzhinin, A. V.; Fedorova, O. V.; Rusinov, G. L.; Charushin, V. N. Pre-organization of diarylideneacetonyl crownophanes in single crystals to photochemical transformations. *Russ. Chem. Bull.* **2011**, *60*, 824−840.

(17) Kuz'mina, L. G.; Vedernikov, A. I.; Howard, J. A. K.; Alfimov, M. V.; Gromov, S. P. Features of styryl dye crystal packings and their influence on [2 + 2] photocycloaddition reaction with single crystal retention. *CrystEngComm* **2015**, *17*, 4584−4591.

(18) Gromov, S. P.; Vedernikov, A. I.; Lobova, N. A.; Kuz'mina, L. G.; Dmitrieva, S. N.; Strelenko, YuA.; Howard, J. A. K. Synthesis, Structure, and Properties of Supramolecular Photoswitches Based on Ammonioalkyl Derivatives of Crown-Ether Styryl Dyes. *J. Org. Chem.* **2014**, *79*, 11416−11430.

(19) Alfimov, M. V.; Gromov, S. P.; Stanislavskii, O. B.; Ushakov, E. N.; Fedorova, O. A. Crown-containing styryl dyes. 8. Cation-dependent concerted [2+2]-autophotocycloaddition of photochromic 15-crown-5 ether betaines. *Russ. Chem. Bull.* **1993**, *42*, 1385−1389.

(20) Biradha, K.; Santra, R. Crystal engineering of topochemical solid state reactions. *Chem. Soc. Rev.* **2013**, *42*, 950−967.
(21) Santra, R.; Garai, M.; Mondal, D.; Biradha, K. Anion Influence in Directing and Altering the Stereochemistry of the Double [2+2] Reaction of Bis-Pyridyl Dienes in their Silver Complexes: A Green Synthetic Route. *Chem. - Eur. J.* **2013**, *19*, 489−493.
(22) Elacqua, E.; Kaushik, P.; Groeneman, R. H.; Sumrak, J. C.; Bučar, D-K.; MacGillivray, L. R. A Supramolecular Protecting Group Strategy Introduced to the Organic Solid State: Enhanced Reactivity through Molecular Pedal Motion. *Angew. Chem., Int. Ed.* **2012**, *51*, 1037−1041.
(23) Santra, R.; Biradha, K. Solid state double [2+2] photochemical reactions in the co-crystal forms of 1,5-bis(4-pyridyl)-1,4-pentadiene-3-one: establishing mechanism using single crystal X-ray, UV and H-1 NMR. *CrystEngComm* **2011**, *13*, 3246−3257.
(24) Vatsadze, S. Z.; Gromov, S. P. Novel Linear Bis-Crown Receptors with Cross-Conjugated and Conjugated Central Cores. *Macroheterocycles* **2017**, *10*, 432−445.
(25) Vatsadze, S. Z.; Gavrilova, G. V.; Zyuz'kevich, F. S.; Nuriev, V. N.; Krut'ko, D. P.; Moiseeva, A. A.; Shumyantsev, A. V.; Vedernikov, A. I.; Churakov, A. V.; Kuz'mina, L. G.; Howard, J. A. K.; Gromov, S. P. Synthesis, structure, electrochemistry, and photophysics of 2,5-dibenzylidenecyclopentanones containing in benzene rings substituents different in polarity. *Russ. Chem. Bull.* **2016**, *65*, 1761−1772.
(26) Kar, S.; Ramamoorthy, G.; Sinha, S.; Ramanan, M.; Pola, J. K.; Golakoti, N. R.; Nanubolu, J. B.; Sahoo, S. K.; Dandamudi, R. B.; Doble, M. Synthesis of diarylidenecyclohexanone derivatives as potential anti-inflammatory leads against COX-2/mPGES1 and 5-LOX. *New. J. Chem.* **2019**, *43*, 9012−9020.
(27) Leong, S. W.; Chia, S. L.; Abas, F.; Yusoff, K. Asymmetrical meta-methoxylated diarylpentanoids: Rational design, synthesis and anti-cancer evaluation in-vitro. *Eur. J. Med. Chem.* **2018**, *157*, 716−728.
(28) Singh, M.; Raghav, N. Synthesis, docking, and in vitro studies of some substituted bischalcones on acid and alkaline phosphatases. *Med. Chem. Res.* **2014**, *23*, 1781−1788.
(29) Zhao, C.; Cai, Y.; He, X.; Li, J.; Zhang, L.; Wu, J.; Zhao, Y.; Yang, S.; Li, X.; Li, W.; Liang, G. Synthesis and anti-inflammatory evaluation of novel mono-carbonyl analogues of curcumin in LPS-stimulated RAW 264.7 macrophages. *Eur. J. Med. Chem.* **2010**, *45*, 5773−5780.
(30) Kuz'mina, L. G.; Vedernikov, A. I.; Gromov, S. P.; Alfimov, M. V. Crystallographic Approach to the [2 + 2] Photocycloaddition Topochemical Reactions of Unsaturated Compounds with Single Crystal Retention. *Crystallogr. Rep.* **2019**, *64*, 691−712.
(31) Tsedilin, A. M.; Fakhrutdinov, A. N.; Eremin, D. B.; Zalesskiy, S. S.; Chizhov, A. O.; Kolotyrkina, N. G.; Ananikov, V. P. How sensitive and accurate are routine NMR and MS measurements? *Mendeleev Commun.* **2015**, *25*, 454−456.
(32) Butcher, R. J.; Jasinski, J. P.; Narayana, B.; Sarojini, B. K.; Bindya, S.; Yathirajan, H. S. 2,5-Bis(3,4-dimethoxybenzylidene)-cyclopentanone. *Acta Crystallogr., Sect. E: Struct. Rep. Online* **2007**, *63*, o3270−o3271.
(33) Vedernikov, A. I.; Basok, S. S.; Gromov, S. P.; Kuz'mina, L. G.; Avakyan, V. G.; Lobova, N. A.; Kulygina, E. Y.; Titkov, T. V.; Strelenko, Y. A.; Ivanov, E. I.; Howard, J. A. K.; Alfimov, M. V. Synthesis and structure of bis-crown-containing stilbenes. *Russ. J. Org. Chem.* **2005**, *41*, 843−854.
(34) Nuriev, V. N.; Fedorov, O. V.; Moiseeva, A. A.; Freidzon, A. Y.; Kurchavov, N. A.; Vedernikov, A. I.; Medved'ko, A. V.; Pod'yacheva, E. S.; Vatsadze, S. Z.; Gromov, S. P. Synthesis, structure, spectral properties, and electrochemistry of bis(crown ether) containing 1,3-distyrylbenzenes. *Russ. J. Org. Chem.* **2017**, *53*, 1726−1737.
(35) Majouga, A. G.; Beloglazkina, E. K.; Moiseeva, A. A.; Shilova, O. V.; Manzheliy, E. A.; Lebedeva, M. A.; Stephen, D. E.; Khlobystov, A. N.; Zyk, N. V. Cleavage of the C-S bond with the formation of a binuclear copper complex with 2-thiolato-3-phenyl-5-(pyridine-2-ylmethylene)-3,5-dihydro-4H-imidazole-4-one. A new mimic of the active site of N_2O reductase. *Dalton Trans.* **2013**, *42*, 6290−6293.
(36) Tsukerman, S. V.; Kutulya, L. A.; Lavrushin, V. F. *Russ. J. Org. Chem.* **1964**, *34*, 3597.
(37) Issa, R. M.; Etaiw, S. H.; Issa, I. M.; El-Shafie, A. K. Electronic Absorption Spectra of some Diarylidene-Cyclopentanones and -Cyclohexanones. *Acta Chim. Acad. Sci. Hung.* **1976**, *89*, 381−391.
(38) Gutrov, V. N.; Zakharova, G. V.; Fomina, M. V.; Starostin, R. O.; Nuriev, V. N.; Gromov, S. P.; Chibisov, A. K. Molecular Photonics of 2,4-Dibenzylidenecyclobutanone and Its Derivatives. *High Energy Chem.* **2020**, *54*, 303−307.
(39) Gutrov, V. N.; Zakharova, G. V.; Fomina, M. V.; Nuriev, V. N.; Gromov, S. P.; Chibisov, A. K. Molecular photonics of dienones based on cycloalkanones and their derivatives. *J. Photochem. Photobiol., A* **2022**, *425*, No. 113678.
(40) Zakharova, G. V.; Zyuz'kevich, F. S.; Nuriev, V. N.; Vatsadze, S. Z.; Plotnikov, V. G.; Gromov, S. P.; Chibisov, A. K. Photonics of Bis(diethylaminobenzylidene)cyclopentanone and Its Analogue with the Bisazacrown Moiety in Acetonitrile. *High Energy Chem.* **2016**, *50*, 27−31.
(41) Al-Anber, M.; Vatsadze, S. Z.; Holze, R.; Lang, H.; Thiel, W. R. π-Conjugated *N*-heterocyclic compounds: correlation of computational and electrochemical data. *Dalton Trans.* **2005**, *51*, 3632−3637.
(42) Vatsadze, S. Z.; Al-Anber, M.; Thiel, W. R.; Lang, H.; Holze, R. Electrochemical studies and semiempirical calculations on pi-conjugated dienones and heterocyclic nitrogen containing donor ligand molecules. *J. Solid State Electrochem.* **2005**, *9*, 764−777.
(43) Bruker. *APEX2, SADABS and SAINT*; Bruker AXS Inc.: Madison, Wiskonsin, USA, 2008.
(44) Dolomanov, O. V.; Bourhis, L. J.; Gildea, R. J.; Howard, J. A. K.; Pushman, H. OLEX2: a complete structure solution, refinement and analysis program. *J. Appl. Cryst.* **2009**, *42*, 339−341.
(45) *SHELXTL-Plus*, version 5.10; Bruker AXS: Madison, Wisconsin, USA, 1997.
(46) Granovsky, A. A. *Firefly*, version 8.2.0, 2019. http://classic.chem.msu.su/gran/firefly/index.html.
(47) Schmidt, M. W.; Baldridge, K. K.; Boatz, J. A.; Elbert, S. T.; Gordon, M. S.; Jensen, J. J.; Koseki, S.; Matsunaga, N.; Nguyen, K. A.; Su, S.; Windus, T. L.; Dupuis, M.; Montgomery, J. A. General atomic and molecular electronic structure system. *J. Comput. Chem.* **1993**, *14*, 1347−1363.
(48) Tomasi, J.; Mennucci, B.; Cammi, R. Quantum Mechanical Continuum Solvation Models. *Chem. Rev.* **2005**, *105*, 2999−3094.
(49) Marenich, A. V.; Cramer, C. J.; Truhlar, D. G. Universal solvation model based on solute electron density and on a continuum model of the solvent defined by the bulk dielectric constant and atomic surface tensions. *J. Phys. Chem. B* **2009**, *113*, 6378−6396.
(50) Laikov, D. N. Fast evaluation of density functional exchange-correlation terms using the expansion of the electron density in auxiliary basis sets. *Chem. Phys. Lett.* **1997**, *281*, 151−156.
(51) Laikov, D. N.; Ustynyuk, Y. A. PRIRODA-04: a quantum-chemical program suite. New possibilities in the study of molecular systems with the application of parallel computing. *Russ. Chem. Bull.* **2005**, *54*, 820−826.
(52) Fomina, M. V.; Kurchavov, N. A.; Freidzon, A. Y.; Nuriev, V. N.; Vedernikov, A. I.; Strelenko, YuA.; Gromov, S. P. Self-assembly involving hydrogen bonds. Spectral properties and structure of supramolecular complexes of bis-aza-18-crown-6-containing dienones with alkanediammonium salts. *J. Photochem. Photobiol., A* **2020**, *402*, No. 112801.

https://doi.org/10.1021/acsomega.1c06129
ACS Omega 2022, 7, 10087−10099